

BOLOMETER SIMULATION USING SPICE

Hollis H. Jones¹

NASA Goddard Space Flight Center, Greenbelt, MD 20771, USA

Shahid Aslam

RITSS, 4400 Forbes Blvd, Lanham, MD 20706, USA

Brook Lakew

NASA Goddard Space Flight Center, Greenbelt, MD 20771, USA

ABSTRACT

A general model is presented that assimilates the thermal and electrical properties of the bolometer—this block model demonstrates the Electro-Thermal Feedback (ETF) effect on the bolometers performance. This methodology is used to construct a SPICE model that by way of analogy combines the thermal and electrical phenomena into one simulation session. The resulting circuit diagram is presented and discussed.

BOLOMETER SIMULATION

General steady-state bolometer model

A general model describing the bolometer operation is presented here. The model can be utilized for normal state and transition edge (TE) types of operation and is not exclusively driven by any particular mathematical expression for the bolometer resistance $R(\Delta T)$, where ΔT is the temperature difference between the bolometer mass and the heatsink. Moreover, the model expounds easy-to-visualize mechanisms and yields simple mathematical statements. The static-state model as shown in Figure 1 is constructed in the usual system form—that is, with the plant, feedback, and summation blocks.

The following briefly describes the process of Figure 1. The input is the optical power Φ into which the electrical or self-heating power P_e is summed. This summation is divided by the thermal conductance G making it the temperature argument for $R(\Delta T)$. The result is then multiplied by the bias current I to produce the output of the plant—in this case, the readout voltage V . The output voltage is in turn multiplied by feedback block I to form P_e , thus demonstrating regenerative feedback. Under proper conditions, an equilibrium point is reached—otherwise, one obtains thermal runaway. In other terms, this model demonstrates the Electro-Thermal Feedback (ETF) effect explicitly.

The configuration of Figure 1 provides two additional features: 1) If no optical power is present, i.e., $\Phi=0$, P_e can bypass the summation block and V gives the equilibrium voltage offset V_e ; and 2) the model depicts a constant current configuration, by substituting V for I (and vice-versa) and reciprocating $R(\Delta T)$, a model is derived that responds to a constant voltage bias operation. With this setup, the load that reads the current, such as a SQUID, must be included.

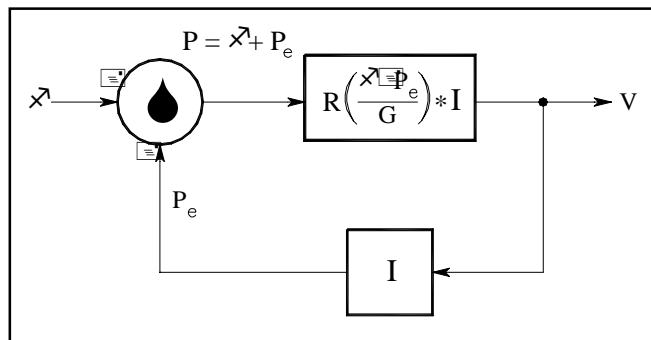


Figure 1. General static-state bolometer model

¹ Contact information for H. H. Jones: Email: holjones@pop500.gsfc.nasa.gov, phone 301-286-5755

To demonstrate the utility of the model, using a normal state expression, $R(\Delta T) = m \cdot \Delta T + R_a$, where m is the slope or the invariant $\alpha_0 R_0$ and R_a is the intercept or resistance at $\Delta T = 0$, one can easily extract a simple output expression from the model such that ΔT is eliminated. The output, assuming constant current, can be shown as, $V = V_\phi + V_e$, where,

$$V_\phi = \frac{\phi}{G} \cdot m \cdot \frac{I_b}{(1-a)} \quad , \quad V_e = R_a \cdot \frac{I_b}{(1-a)} \quad \text{and} \quad a = \frac{m \cdot I_b^2}{G} \quad (1)$$

In Eq. (1), V_ϕ is that part of the output voltage due to the applied optical signal—the responsivity—and V_e is that part due to the offset voltage at ETF equilibrium.

PSPICE model

The Simulation Program with Integrated Circuit Emphasis (SPICE) program has the ability to simulate both thermal and electrical properties—these authors use PSPICE. By way of analogy, current and voltage represent heat flow Q and temperature differences ΔT respectively. Other authors have revealed this technique. For example, Yvon and Sushkov¹ and Shie, *et. al.*², used SPICE models to emulate normal state bolometer circuits.

The model realized here relies on an otherwise unknown $R(\Delta T)$ as shown in Figure 1, but note that PSPICE does not allow passive devices to be varied during a simulation session. They can be changed via a *.step* command for each session run, but this is a very tedious activity. However, as Figure 2 shows, any resistor can be modeled as a Voltage Controlled Voltage Source (VCVS) or a Voltage Controlled Current Source (VCCS) for a constant current or a constant voltage bias-mode operation, respectively. Using the VALUE option in the statement allows one to use a mathematical expression that can contain voltage nodes or currents through other devices.

Focusing only on the VCVS, by analogy, $R(VT1 - VT2)$ is a $R(\Delta T)$ equation where $VT1$ and $VT2$ represent the temperatures developed at the bolometer mass and the heatsink, respectively. Note that in Figure 2, the statement $R(VT1 - VT2)$ is not a valid PSPICE construct, it represents the function that will describe the actual $R(\Delta T)$. This function is multiplied by the current flowing through the source rendering a voltage drop across the VCVS device.

Figure 3 gives a simple PSPICE circuit for a constant current-mode normal state bolometer circuit in which the VCVS from Figure 2 has been inserted. On the left side is the thermal loop with its device analogues

whereas on the right side is the electrical loop with its components. Examining Figure 3 left-to-right, the independent current source *Iphi* symbolizes the optical signal power—the current represents this power. In parallel with this, the VCCS, *Getf*, emulates the ETF effect by injecting current into the junction. This current is determined by the statement $V(10) \cdot I(Vbo)$, where $V(10)$ is the bolometer element voltage drop and $I(Vbo)$ is the current into the element. The resistor device *RG* acts as the thermal conductance G . Its value is the reciprocal of G . The voltage across *RG* emulates the

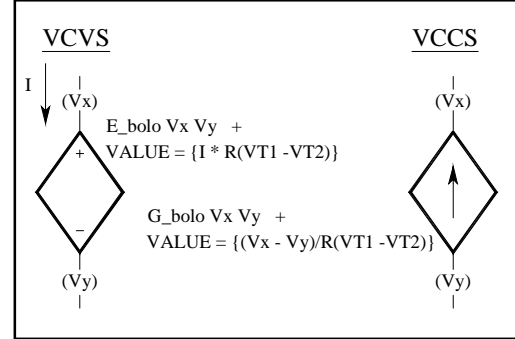


Figure 2. SPICE resistance emulation devices

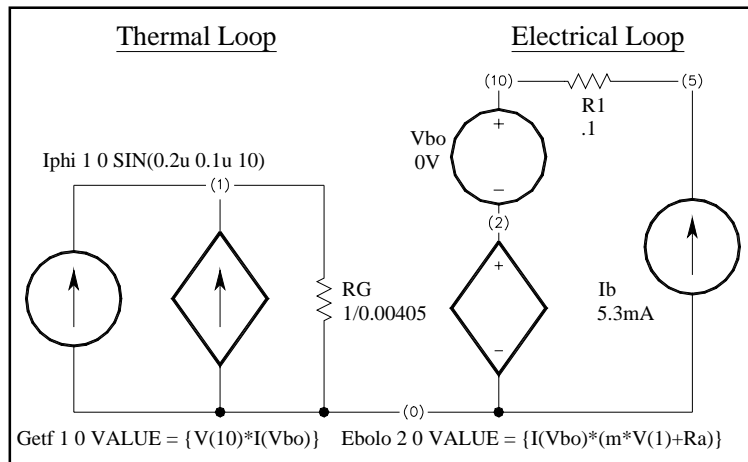


Figure 3. Static-state SPICE diagram for bolometer circuit in constant current mode

temperature difference ΔT and controls **Ebolo**. In series is **Vbo**, a 0-volt source used to measure the current through **Ebolo**. The placement of resistor **R1** not only serves as a topology resistance but also can be increased in value to yield a voltage divider scheme in the circuit. The independent current source **Ib** provides the necessary constant bias current. The output voltage is determined, for the values shown in Figure 3 or for a voltage divider scheme, by the nodes on either end of the VCVS **Ebolo**—that is, at nodes 10 and 0.

Noise voltage and current sources can be inserted for complete sensor/readout simulation, but these are not options in PSpice—that is, the package does not contain random generators. It does allow one to obtain thermal noise spectral density for every resistor and/or calculate shot and $1/f$ spectral densities for every semiconductor device. In both cases, when the `.noise` statement included in the circuit file, the results are presented only in the frequency domain. Motchenbacher and Connelly³ and Fish⁴ dedicate entire chapters to methods in which noise voltage and current source of various categories can be constructed in SPICE, such as $1/f$ noise, excess, and amplifier noise. In addition, post-processing measurement techniques for spectral densities noise bandwidths are covered.

Figure 4 depicts an example voltage noise source (shot noise) containing a $1/f$ component that can be constructed and inserted into Figure 3 as a subcircuit. The amplitude and order can be modified by adjusting the current source **In** and the parameters of the `.model` statement for the diode **Dn**. Parameter KF is the $1/f$ noise coefficient in amps and parameter AF is the $1/f$ exponent. Other subcircuits can be constructed that produce Johnson or resistor excess noise also containing $1/f$ spectral noise.

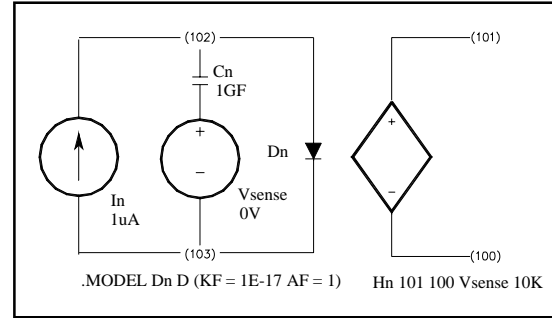


Figure 4. SPICE noise source with $1/f$ component

Simulation test

To test the simulation, Figure 3 is modified to reflect an actual measurement setup so that the effective thermal conductance as well as the actual static thermal conductance can be extracted. Figure 5 shows the

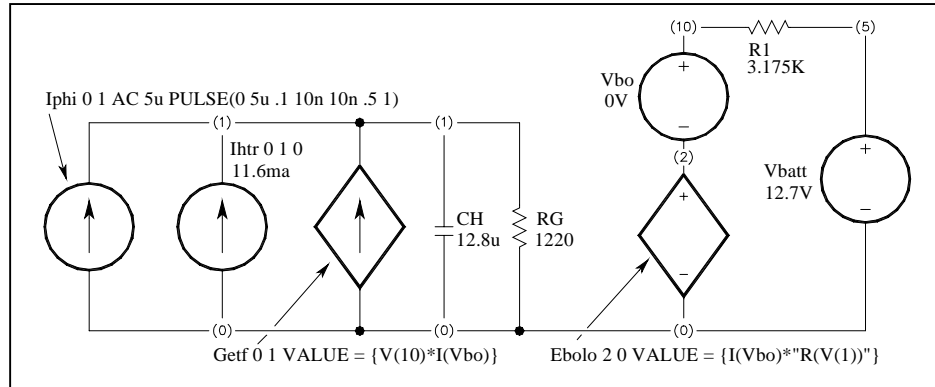


Figure 5. Simulation diagram of measurement setup

modified diagram with the constant current source replaced with a 12.7V battery (**Vbatt**) and **R1** increased to 3.175K Ω in order to present a nearly constant current of 4.0mA to the bolometer element. A closed-form functional equation⁵ is used in **Ebolo**. A thermal capacity⁶ **CH** of 12.8 μ J/K as well as the current source **Ithr** to represent heater energy to maintain the operating point is inserted into the thermal loop. Thermal resistance **RG** was iteratively adjusted until the effective time constant of the output was at 90ms. A value of 1220 Ω was found that represents a thermal conductance of ~ 0.820 mW/K. An effective conductance of 0.142mW/K was derived from the time constant. **Iphi** is configured to produce a square wave optical signal of 5 μ W peak-to-peak. This produces the resulting exponential waveform at the voltage output node 10 as depicted by Figure 6. Larger values of optical signal eventually distort the waveform as the resistance slope

at the TE region becomes less a straight-line slope and more an exponential shape. A frequency spectrum result is shown in Figure 7. A sinusoid optical signal is swept from 1mHz to 100Hz at 5 μ W rms. The result not only demonstrates the high responsivity acquired (> 1000) in the TE region but also confirms the time constant value due to the half-power point of ~ 1.7 Hz.

CONCLUSION

A general model is demonstrated that portrays the thermal and electrical properties of the bolometer. The model is one that can be used for all steady state configurations—current or voltage bias modes. A PSPICE simulation model for steady state configurations was considered with a brief examination of a dynamic state modeling. Furthermore, information about noise modeling was disseminated. Amplifier components, such as opamps and transformers, can also be inserted into Figures 3 or 5 for complete readout/sensor simulation. Moreover, by replacing the VCVS (*Ebolo*) with a VCCS (*Gbolo*) and *Ib* with an independent voltage source, simulation models of Figures 3 and 5 can be rearranged to perform as a constant voltage-bias bolometer circuit.

REFERENCES

1. D. Yvon, V. Sushkov, *Low Noise Cryogenic Electronics: Preamplifier Configurations with Feedback on the Bolometer*, IEEE Transactions on Nuclear Science, Vol. 47, No. 2, April 2000.
2. J. Shie, Y. Chen, *et. al.*, *Characterization and Modeling of Metal-Film Microbolometer*, Journal of Micromechanical Systems, Vol. 5, No. 4, December 1996.
3. C.D. Motchenbacher, J.A. Connelly, *Low Noise Electronic System Design*, John Wiley and Sons, New York, NY, 1993.
4. P. J. Fish, *Electronic Noise and Low Noise Design*, McGraw-Hill, New York, NY, 1994.
5. H.H. Jones and S. Aslam, private communication, May, 2003.
6. J. Brasunas, private communication, March, 2000.

